C. R. Mecanique 341 (2013) 191–200

Contents lists available at SciVerse ScienceDirect

Comptes Rendus Mecanique

www.sciencedirect.com

Combustion, flow and spray dynamics for aerospace propulsion

Experimental analysis of laser-induced spark ignition of lean turbulent premixed flames

Céline Cardin *, Bruno Renou, Gilles Cabot, Abdelkrim Boukhalfa

CORIA, UMR 6614, Université et INSA de Rouen, BP 8, 76801 Saint-Etienne du Rouvray cedex, France

ARTICLE INFO

Article history:
Available online 5 January 2013

Keywords:
Laser-induced spark ignition
Flame kernel propagation
Turbulent flame

Mots-clés :
Allumage par étincelle induite par laser
Propagation de noyau de flamme
Flamme turbulente

ABSTRACT

Spark ignition in lean and highly turbulent premixed flows is experimentally investigated by measuring the Minimum Ignition Energy (MIE), for laser-induced spark ignition in methane/air mixtures, as a function of the velocity fluctuation u', the equivalence ratio and the focal length of the focusing lens. The burner provides a 2D stationary flow with a homogeneous and isotropic turbulence.

A clear transition on the MIE values is observed, when u' increases. Before the transition, the MIE increases gradually with u', whereas across the transition (for $u' \sim 1\ \mathrm{m\,s^{-1}}$), the MIE increases strongly. As the MIE is proportional to the flame thickness to the power of three, this slope breakdown could indicate the existence of two distinct modes of flame structure. From a certain threshold of turbulence intensity, the flame kernel no longer develops in a flamelet regime, rather in a regime where its structure is strongly modified by the turbulence: the flame front would undergo an intense mixing by all the eddies of the flow ($Da < 1$) and a thickening by the small eddies ($Ka \sim 10$), leading to an intense stretch and possibly local extinctions. This ignition transition phenomenon in turbulent mixtures has already been reported by Shy et al. (2010) [1] and Huang et al. (2007) [2], but for different experimental conditions.

The present study also reveals that there is a common criterion for the ignition transition phenomenon: whatever the focal length of the focusing lens and the equivalence ratio of the mixture, an ignition transition occurs when the turbulent flow reaches a Karlovitz number of the order of 10.

RÉSUMÉ

L'allumage par étincelle dans des écoulements prémélangés pauvres et fortement turbulents est étudié expérimentalement en mesurant l'Energie Minimum d'Allumage (MIE, Minimum Ignition Energy), dans le cas de l'allumage par étincelle induite par laser de mélanges méthane/air, en fonction de la fluctuation turbulente de vitesse u', de la richesse et de la distance focale de la lentille de focalisation. Le brûleur fournit un écoulement 2D stationnaire, avec une turbulence homogène et isotrope.

Les valeurs de la MIE présentent une transition nette, quand u' augmente. Avant la transition, la MIE augmente lentement avec u', tandis qu'après la transition (pour $u' \sim 1\ \mathrm{m\,s^{-1}}$), la MIE augmente très rapidement. Comme la MIE est proportionnelle à l'épaisseur de flamme à la puissance trois, cette rupture de pente pourrait indiquer l'existence de deux modes distincts de structure de flamme. A partir d'un certain niveau d'intensité turbulente, le noyau de flamme ne se développe plus dans un régime de flammelettes, mais dans un régime où sa structure est fortement modifiée par la turbulence : le front de flamme est

* Corresponding author.
E-mail addresses: cardin@coria.fr (C. Cardin), renou@coria.fr (B. Renou), cabot@coria.fr (G. Cabot), boukhalfa@coria.fr (A. Boukhalfa).

1631-0721/$ – see front matter
http://dx.doi.org/10.1016/j.crme.2012.10.019

soumis à un mélange intense de la part de tous les tourbillons de l'écoulement ($Da < 1$) et à un épaississement par les petites structures turbulentes de l'écoulement ($Ka \sim 10$), conduisant à des étirements intenses et éventuellement à des extinctions locales. Ce phénomène de transition d'allumage dans des mélanges turbulents a déjà été observé par Shy et al. (2010) [1] et Huang et al. (2007) [2], mais pour des conditions expérimentales différentes.

La présente étude montre également l'existence d'un critère commun pour le phénomène de transition d'allumage : quelles que soient la distance focale de la lentille de focalisation et la richesse du mélange, une transition d'allumage est observée quand l'écoulement turbulent atteint un nombre de Karlovitz de l'ordre de 10.

1. Introduction

Lean turbulent combustion is a fundamental subject in combustion science [3,4] and is encountered in many applications, such as car or aeronautical engines [5]. However, in this field, many problems are still observed. The increase of the levels of turbulence and the reduction of the introduced fuel quantities are at the origin of instabilities [3] which can lead to difficulties to stabilize the flame on the burner. Local extinctions in the flame front can occur, leading to pollutant production (HC, CO) [6], and problems of ignition are also encountered. The understanding and the predictability of the ignition in such devices are strengthened by the two-phase nature of the flow (where fuel is injected), the flow complexity as well as the turbulent mixing. To simplify the operating conditions and perform parametrical studies, some experimental and numerical studies have been developed in simpler configurations to study the ignition of a flame kernel and its propagation (the early stages) in laminar or turbulent flows.

Ignition of fuel/air flows has been the subject of numerous studies [7–9]. In laminar flows, ignition mechanisms are well known [10]. However, when the flow becomes very turbulent, the flame kernel is subjected to a high turbulent dissipation, leading to an increase of the Minimum Ignition Energy (MIE) [11], and also at the origin of mechanisms modifying the flame structure. Thus, in turbulent flows, ignition is more complex and some questions are still open.

The recent studies of Shy et al. [1,2] report an ignition transition phenomenon in turbulent mixtures, based on the measurements of the MIE of lean turbulent premixed flames as a function of the velocity fluctuation u'. First, the MIE increases gradually with the velocity fluctuation, then, from a certain threshold ($Ka \sim 10$) depending on the equivalence ratio, the MIE increases abruptly. The authors explain that this ignition transition indicates the existence of two distinct modes of ignition, corresponding to the transition between the flamelet regime and the broken reaction zones regime. These MIE measurements are obtained thanks to ignition by electric sparks, in a cruciform explosion bomb, in which an isotropic and homogeneous turbulence is generated by two counter-rotated fans. This study raises the following question: does this phenomenon of ignition transition depends on the experimental conditions of the study, or is it a universal phenomenon.

The present study contributes to the analysis of spark ignition, in lean and highly turbulent premixed flows. Different parameters influencing the initiation and the propagation mechanisms of the flame kernel are studied, for laser-induced spark ignition in methane/air mixtures, by measuring the MIE as a function of the turbulent flow properties (mainly u'), the equivalence ratio (Φ) and the volume of energy deposition (depending on the focal length f of the focusing lens). It is important to note that the MIE is the energy required to ignite a self-sustained flame kernel, with an ignition probability equal to 50%. The burner provides a steady 2D flow, with a homogeneous and isotropic turbulence generated over a wide range of intensities, thanks to different turbulence grids.

From these experimental results, the ignition transition phenomenon in turbulent mixtures is discussed over a broad range of experimental conditions, in terms of ignition system, flows properties and turbulence intensity.

2. Experimental set-up

2.1. The wind-tunnel facility

Air and methane flows, regulated by two mass flow controllers (Bronkhorst), are injected and mixed in the wind-tunnel, before being directed to a vertical divergent–convergent chamber composed of glass ball bed, honeycomb and screens, to attenuate residual turbulent perturbations, as shown on Fig. 1. The convergent, which has a (11 : 1) contraction ratio and a 8 cm square exit section, provides a laminar and stationary flow, with a flat velocity profile of amplitude 4 $\mathrm{m\,s^{-1}}$.

2.2. The turbulence generators

To generate a homogeneous and isotropic turbulence with a wide range of intensities, different grids are placed at the exit of the convergent. Relatively low turbulence intensities are generated thanks to three grids (B, E, F), whose main characteristics are displayed in Table 1. M and σ are respectively the mesh size and the blockage ratio. E- and F-grids are perforated plates, with a hole diameter equal to D, whereas B-grid is constituted by round rods with a 2 mm diameter.

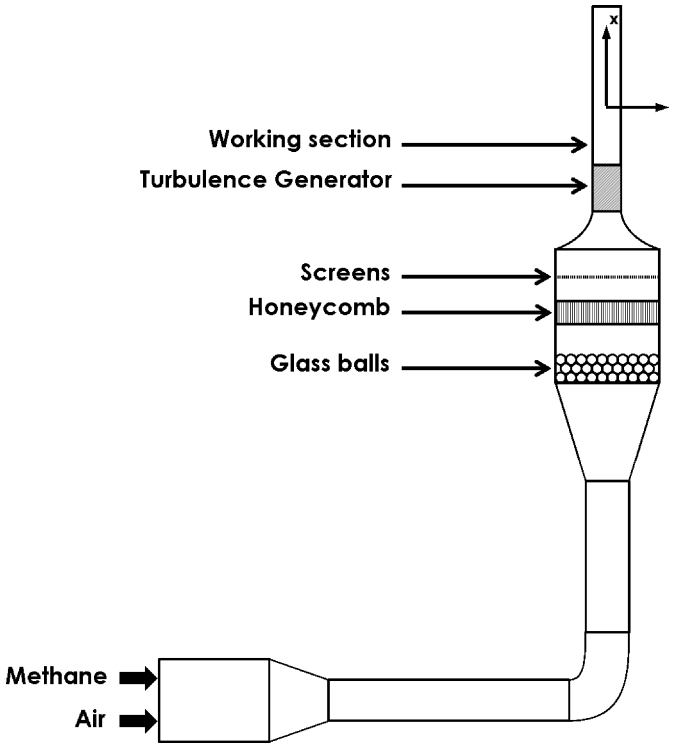

Fig. 1. The wind-tunnel facility.

Table 1
Main characteristics of the turbulence generators (M: mesh size, σ: blockage ratio, D: hole diameter).

		M (mm)	σ (%)	D (mm)
	Grid B	5	64	/
	Grid E	8	69	5
	Grid F	13	56	10
	Plate 1	4	49	3
MuSIG	Plate 2	9	60	6
	Plate 3	24.7	67	15

High turbulence intensities are generated thanks to the multi-scale injection grid (MuSIG) developed by Mazellier et al. [12]. This turbulence generator, which allows to reach a high turbulence by conserving homogeneity and isotropy properties, is constituted by three perforated plates, whose mesh size, hole diameter and blockage ratio increase along the flow. Table 1 displays the characteristics of the three plates. The spacing between the plates j and $j+1$ is equal to $L_j = 3.5M_j$, corresponding to the distance from the plate j where the turbulent kinetic energy reaches a maximum.

The turbulent properties induced in the flow by these several turbulence generators are displayed in Table 2, as a function of the height h above the B-, E- and F-grids or above the last grid of the MuSIG. r is the global isotropy factor, defined as $r = u'/v'$, where u' and v' are the velocity fluctuation respectively calculated along the x-axis and the y-axis. The axial velocity U, the integral length-scale L_i and the Kolmogorov scale η_k are also given in Table 2. Thus, by realizing ignition trials in the conditions displayed in Table 2, MIE can be measured over a wide range of turbulence intensity, varying from 34.2 to 3.7%.

2.3. The ignition system

Fig. 2 displays a top view of the ignition and the measurement systems. Ignition are performed thanks to laser-induced sparks, generated by a Nd:YAG laser (Quanta-Ray Pro, Spectra-Physics) which operates as a Q-switched laser and which has a nominal energy equal to 500 mJ/pulse. The beam delivered by the laser has a pulse width (FWHM) of 8 ns, a wavelength of 532 nm, a frequency of 10 Hz, a diameter of 10 mm and a divergence of 0.5 mrad.

In order to generate a spark in the methane/air flow, a plano-convex lens focuses the laser beam at a given height above the turbulence generator. The volume of energy deposition corresponds to volume of the laser beam at the focal point and

Table 2
Turbulent properties generated by the several turbulence generators.

	h (mm)	U (m/s)	u' (m/s)	r	L_i (mm)	η_k (μm)
MuSIG	60	6.71	2.05	1.21	4.90	49
	70	6.01	1.71	1.19	4.96	52
	80	5.52	1.43	1.18	5.21	56
	90	5.18	1.21	1.16	5.58	62
	100	4.95	1.05	1.15	6.02	69
	120	4.71	0.83	1.14	7.00	81
	144	4.57	0.68	1.13	8.10	92
	164	4.46	0.60	1.12	8.87	99
Grid F	80	3.59	0.57	1.07	4.32	97
	100	3.59	0.44	0.99	5.06	124
	140	3.59	0.31	0.93	6.17	168
Grid E	140	3.14	0.21	0.92	6.35	224
Grid B	136	3.75	0.14	1.04	5.68	299

Table 3
Volume of energy deposition calculated for different focal lengths of focusing lens.

f (mm)	r (μm)	l (μm)	VED (μm^3)
75	2.540	116.5	2.361E+03
100	3.387	207.1	7.463E+03
150	5.080	466.0	3.778E+04

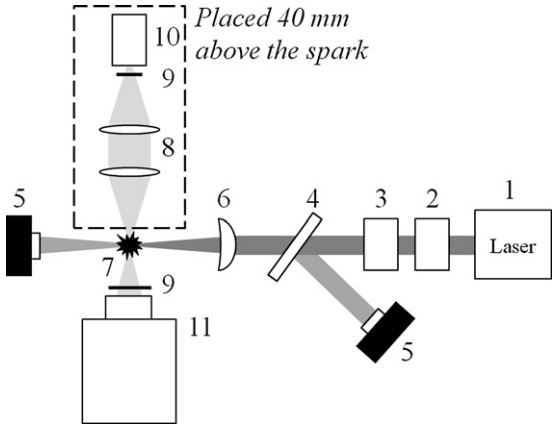

Fig. 2. The measurement and the ignition systems (top view). (1) Nd:YAG laser. (2) Attenuator. (3) Shutter. (4) Beam splitter. (5) Energy meter. (6) Focusing lens. (7) Spark location. (8) Two lenses afocal system. (9) CH filter. (10) Photomultiplier tube. (11) Intensified camera and lens.

differs from the volume of the spark. By assuming that the beam is cylindrical with a Gaussian beam profile, the radius r and the length l of the volume of energy deposition are defined as:

$$r = \left(\frac{2\lambda}{\pi}\right)\left(\frac{f}{d}\right) \tag{1}$$

$$l = (\sqrt{2}-1)\frac{\theta}{d}f^2 \tag{2}$$

where λ, d and θ are respectively the wavelength, the diameter and the divergence of the laser beam. f is the focal length of the focusing lens. To study the influence of the volume of energy deposition on the ignition process, three different focal lengths ($f = 75$ mm; 100 mm; 150 mm) are used. The volume of energy deposition (VED), its radius and its length are given as a function of the focal length in Table 3.

Moreover, an attenuator and a shutter allow one to modify respectively the pulse energy thanks to a rotating beam splitter, and the pulse frequency thanks to a rotating mirror, without modifying the setting of the laser.

2.4. The measurement system

To measure the incident and the deposited energies in the methane/air mixture, a beam splitter (Melles Griot, 16 BPB153 523–532 nm) and two energy meters (Ophir, PE25-DIF) are used (Fig. 2). A small amount ($\sim 14\%$) of the laser beam is

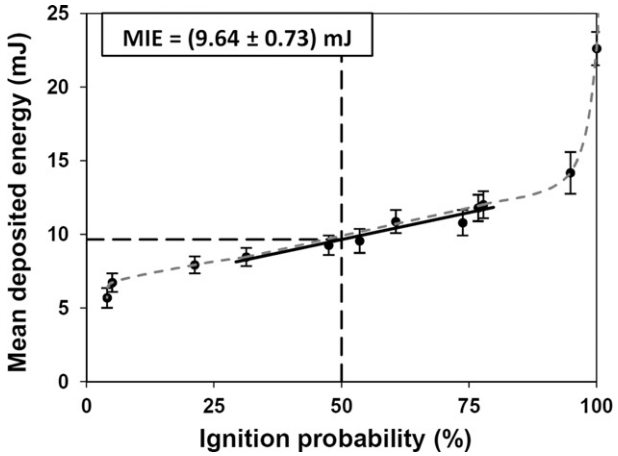

Fig. 3. Measurement of the mean deposited energy as a function of the ignition probability, for the determination of the MIE (MuSIG – $h = 80$ mm, $f = 100$ mm, $\Phi = 0.60$).

reflected by the beam splitter toward the first energy meter. Thanks to a calibration, the measurement of this small portion of energy allows to know the value of the incident energy sent to the focal point. The second energy meter measures the rest of energy which has not been absorbed in the spark at the focal point. Thus, the deposited energy in the mixture can be deduced from the measurement of the two energy meters, which allows the determination of the MIE.

To obtain the MIE, the deposited energy in the mixture has to be recorded, but the success or the failure of the flame kernel initiation also has to be known, at each ignition trial. Thus, an afocal system constituted by two lenses ($f = 200$ mm), a CH filter (Melles Griot, BG12) and a photomultiplier tube (Hamamatsu, 6780-20) with a pinhole of 2 mm diameter, collect the temporal evolution of light (CH radical emission), emitted by the flame kernel 40 mm above the spark, a few milliseconds after the laser pulse (Fig. 2). Thanks to this device, the success or the failure of an ignition trial can be determined. Consequently, by averaging one hundred ignition trials in a fixed configuration, the ignition probability can be obtained for a mean deposited energy. By repeating this operation for different deposited energies, the curve displaying the mean deposited energy in the methane/air mixture as a function of the ignition probability can be plotted, as shown on Fig. 3. Thus, each point comes from 100 laser shots at a constant mean energy. From the energy meters, the energy fluctuations can be also provided and are reported in terms of error bars in Fig. 3. Finally, the MIE, defined as the ignition energy having 50% successful ignitability [13], can be obtained by the interpolation of this curve. For an accurate determination of the MIE, the curve must be plot with about ten points, which corresponds to one thousand ignition trials.

Finally, to study the influence of the volume of energy deposition on the ignition process, an intensified camera with a gate of 4 ns (Princeton Instruments – Roper Scientific – GENII 512×512 pixels^2) equipped with a lens (Canon – 65 mm Macro – $f/2.8$ 1–5×) and a bandpass filter centered around 431 nm (Melles Griot, BG12) records images of laser-induced sparks 10 ns after the breakdown (Fig. 2). It corresponds to the time after the breakdown for which the mean intensity of the spark recorded with the ICCD is maximum. In this way, by using a threshold determined from the Otsu's method [14], the spark volume is measured, as a function of the focal length of the focusing lens and the deposited energy at the focal point. A typical recording of plasma image is given in Fig. 7.

3. Results and discussion

3.1. Measurement of the MIE as function of the velocity fluctuation u'

Fig. 4 displays the evolution of the MIE of a methane/air mixture as a function of u'. From the error bars available in Fig. 3, minimum and maximum deposited energies leading to a 50% of ignition probability can also be obtained and reported in Fig. 4 through the error bars. Sparks are created by a lens of a 100 mm focal length and the mixture has an equivalence ratio equal to 0.6. The MIE is normalized by MIE_0, the MIE value in the laminar flow ($\mathrm{MIE}_0 = 3.95$ mJ for $\Phi = 0.60$). According to Fig. 4, the MIE increases as a function of u'. This trend is in good agreement with previous studies dealing with ignition in turbulent flows [1,2,11]. Indeed, when u' raises, the flame kernel is subjected to a higher turbulent dissipation, leading to an increase of the MIE.

Fig. 4 also displays a clear transition on the values of $\mathrm{MIE}/\mathrm{MIE}_0$ when u' increases. The sensitivity for the determination of the u' transition has been checked by using two methodologies: intersections from bi-linear interpolations (least square methods) on 3 and 4 points. The difference in the results leads to an accuracy on the transition less than 0.1 m/s. This transition has already been reported by Shy et al. [1] for different flow conditions and turbulence properties, for a broader range of u' values and for a different ignition system. On Fig. 4, the MIE measurements describe linear slopes, with a change in slope (for $u' \sim 1$ m/s) which could be due to the transition between two distinct modes of flame structures. Indeed, according to Glassman [15], the MIE is proportional to δ^3, where δ is the local flame thickness.

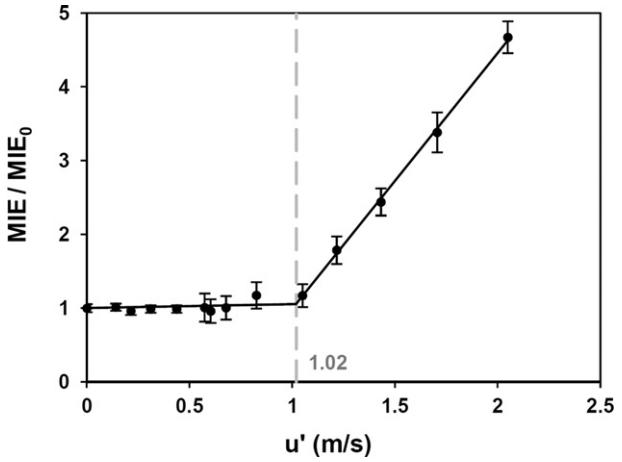

Fig. 4. MIE measurement of a methane/air mixture as a function of u' ($f = 100$ mm, $\Phi = 0.60$). The MIE is normalized by MIE_0, the MIE value in the laminar flow ($MIE_0 = 3.95$ mJ for $\Phi = 0.60$).

Before the transition, for low levels of turbulence, the structure of the flame kernel would be close to a laminar structure; the flame front is wrinkled by turbulent motions, but the inner flame structure remains similar to the laminar flame structure. Thus, in this flamelet regime, the MIE is comparable to the laminar value MIE_0 and increases slightly with u'.

Whereas, after the transition, for higher levels of turbulence, eddies would become sufficiently energetic and small to disturb efficiently and modify the inner flame front structure, in the first stages of the development of the kernel. According to the turbulent combustion diagram, when the Karlovitz number, defined by $Ka = (L_i/\delta_L)^{-1/2} \cdot (u'/S_L)^{3/2}$ (where δ_L and S_L are respectively the thermal flame thickness and the laminar flame velocity and L_i is the integral length-scale), becomes higher than 1, Kolmogorov scales are able to thicken the flame preheat zone, leading to intense stretch and possibly local extinctions. However, a significant change in the combustion regimes is actually observed when the Karlovitz number is of the order of 100, which corresponds to the thickening of the flame reaction zone by the Kolmogorov scales [16]. The Karlovitz number calculated at the transition on Fig. 4 is of the order of 10, but this result is in good agreement with that of Shy et al. [1]. Moreover, the Damköhler number, defined by $Da = (L_i S_L)/(\delta_L u')$, is of the order of 1 ($Da = 0.66$) at the transition on Fig. 4, meaning that the flame chemical time is larger than the turbulent time of all the eddies. Thus, the flame front is submitted to a fast mixing by all the turbulent scales.

Thus, since the MIE is proportional to δ^3 [15], an ignition transition occurs from a certain threshold of turbulence, because the flame kernel would not develop anymore in a flamelet regime, but in a regime where it would be strongly modified by the turbulence motions. The flame front would undergo a thickening by the small eddies ($Ka \sim 10$) and an intense mixing by all the eddies of the flow ($Da < 1$). Consequently, the significant modifications of the flame structure induced by the turbulence would explain the abrupt increase of the MIE as a function of u', for high levels of turbulence.

In the following parts, the phenomenon of ignition transition in turbulent mixtures is studied in other conditions, in terms of equivalence ratios and volumes of energy deposition.

3.2. Influence of the equivalence ratio on the ignition transition

Fig. 5(a) displays the MIE/MIE_0 values plotted as a function of u', for three equivalence ratios ($\Phi = 0.58; 0.60; 0.65$), with sparks created by a lens of 100 mm focal length. It has to be noted that, the leaner the mixture, the more the MIE increases. This trend is in good agreement with previous works measuring the MIE as a function of the equivalence ratio [10,17]. Indeed, for leaner mixtures, less exothermic reactions occur and thus, the flame kernel releases less energy to allow its growth in a self-sustained manner. Consequently, ignition of lean mixtures requires that a higher energy is deposited in the flow, to assist the flame kernel during the first stages of its development.

Moreover, the MIE measurement displays an ignition transition, for the three equivalence ratios. The influence of the equivalence ratio on the ignition transition has also been studied, using others focal lengths of focusing lens ($f =$ 75 mm; 150 mm). The results are displayed on Fig. 5(b), where the values of $u'_{critical}$, that is to say values of u' for which an ignition transition is observed, are plotted as a function of the equivalence ratio. For a fixed focal length of lens, ignition transition occurs for higher levels of turbulence, when the equivalence ratio increases. Indeed, when increasing the equivalence ratio (for lean flames), the increase of the flame temperature involves an increase of the viscosity of the flame front, which can lead to a more intense phenomenon of relaminarization at the origin of a faster dissipation of eddies. Consequently, when increasing the equivalence ratio, higher levels of turbulence must be reached to observe an ignition transition, in order that the flow contains sufficiently small and energetic eddies, able to thicken and modify the flame front structure, before that the phenomenon of dissipation happens.

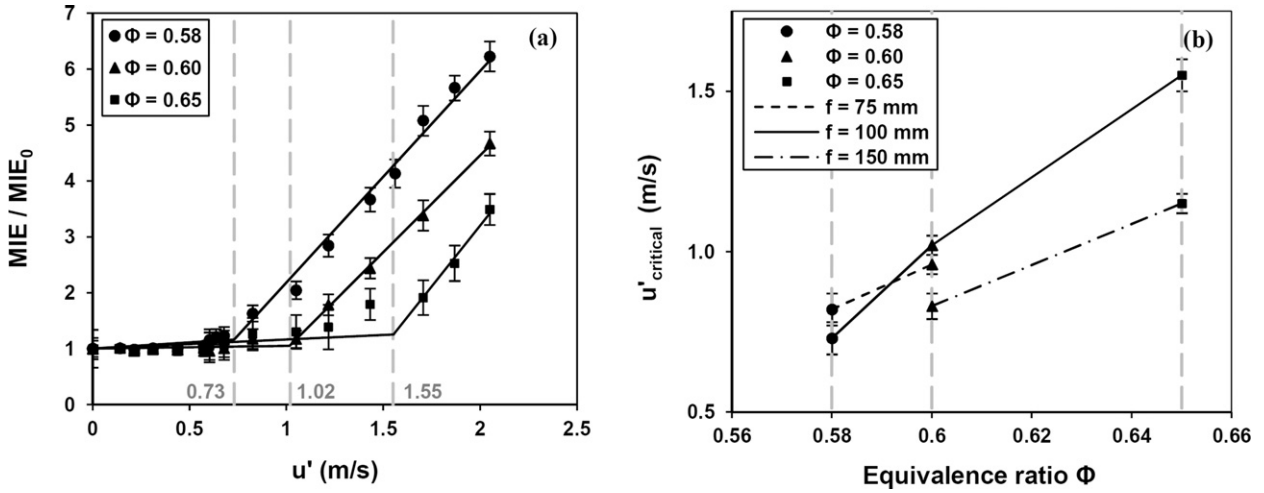

Fig. 5. (a) MIE measurement of a methane/air mixture as a function of u' ($f = 100$ mm, $\Phi = 0.58; 0.60; 0.65$). The MIE is normalized by MIE_0, the MIE value in the laminar flow ($MIE_0 = 4.70$ mJ; 3.95 mJ; 2.09 mJ, respectively for $\Phi = 0.58; 0.60; 0.65$). (b) Values of u' for which an ignition transition is observed, as a function of the equivalence ratio, for three focal lengths of focusing lens ($f = 75$ mm; 100 mm; 150 mm).

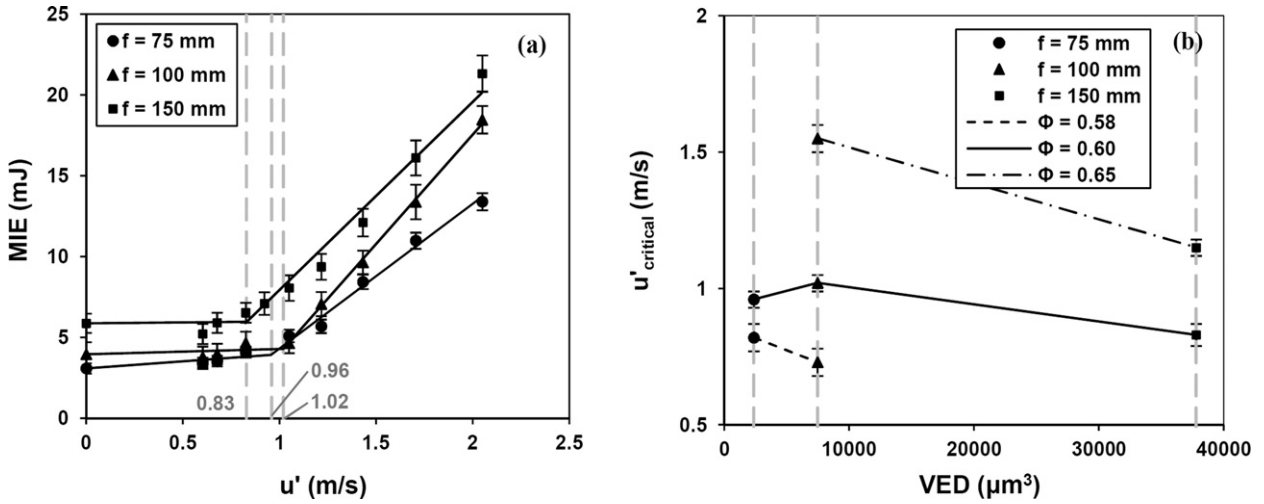

Fig. 6. (a) MIE measurement of a methane/air mixture as a function of u' ($\Phi = 0.60$, $f = 75$ mm; 100 mm; 150 mm). (b) Values of $u'_{critical}$ as a function of the VED of the focusing lens, for three equivalence ratios ($\Phi = 0.58; 0.60; 0.65$).

3.3. Influence of the volume of energy deposition on the ignition transition

To study the influence of the volume of energy deposition (VED) on the ignition mechanisms, the MIE is measured for different focal lengths of the focusing lens ($f = 75$ mm; 100 mm; 150 mm). Indeed, according to Eqs. (1) et (2) previously defined, the VED is proportional to the focal length to the power of four. The results are reported on Fig. 6(a), for a methane/air mixture with an equivalence ratio equal to 0.60. According to Fig. 6(a), reducing the focal length and thus, the VED, leads to a decrease of the MIE, in accordance with previous studies [10]. Moreover, the MIE measurement displays an ignition transition, for the three values of the VED. The influence of this volume on the ignition transition is also studied, for two others equivalence ratios ($\Phi = 0.58; 0.65$). The results are displayed on Fig. 6(b), where $u'_{critical}$ is plotted as a function of the VED, whose values were previously calculated in Table 3. Despite the $u'_{critical}$ value obtained when $\Phi = 0.6$ and VED $= 2400$ μm^3 ($f = 75$ mm), an ignition transition seems to occur for higher levels of turbulence, when the VED decreases, for a fixed equivalence ratio.

Consequently, the reduction of the VED (the focal length) leads to a decrease of the MIE and an increase of the $u'_{critical}$. Indeed, for a fixed incident energy, the reduction of this volume enables one to increase of the incident energy per unit of volume at the focal point, which allows the deposition of a higher energy per unit of volume. This phenomenon is confirmed by the measurement of the spark volume (100 recordings for each condition) as a function of the deposited energy for the three focal lengths, thanks to the intensified camera. On Fig. 7, the spark energy density which corresponds to the ratio between the deposited energy and the mean spark volume is reported as a function of the deposited energy for the three

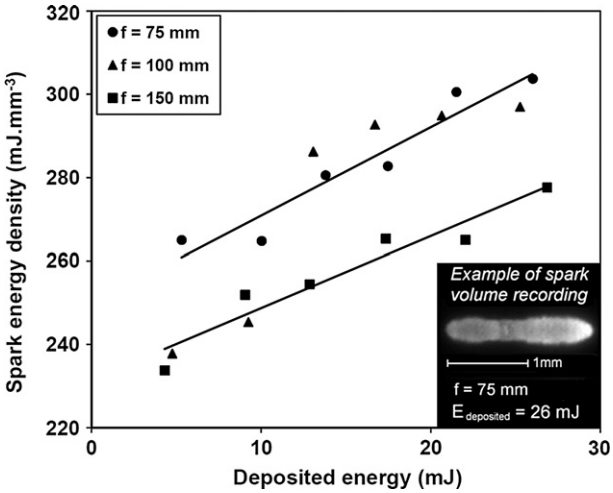

Fig. 7. Spark energy density as a function of the deposited energy for three focal lengths of focusing lens.

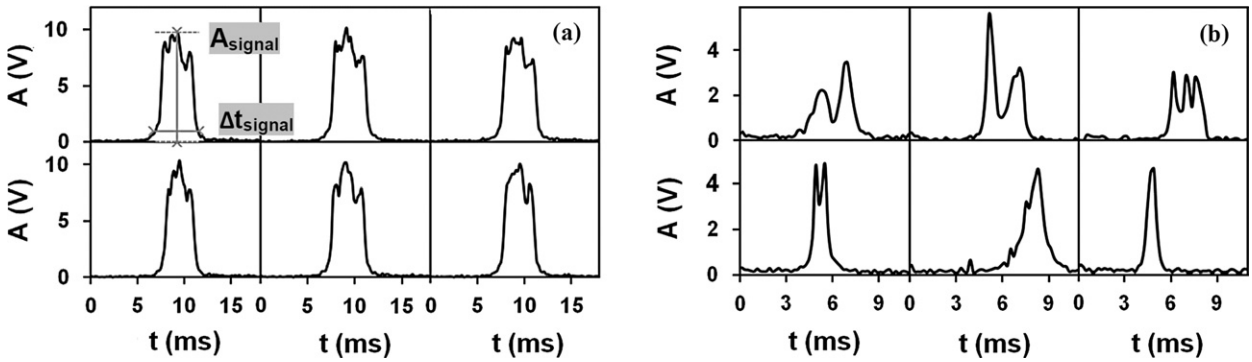

Fig. 8. Examples of signals recorded by the PMT during successful ignitions ($f = 100$ mm, $\Phi = 0.58$) (a) in a laminar flow: $E_{deposited} = 4.8$ mJ, ignition probability = 59.6%, (b) in a very turbulent flow ($u' = 2.05$ m/s): $E_{deposited} = 30.0$ mJ, ignition probability = 55.6%.

focal lengths of lens. A linear fitting is performed for the results obtained for $f = 75$ mm and $f = 150$ mm. An example of spark volume recording is also displayed. As expected, for a given deposited energy, a higher energy per unit of volume is contained in the spark, when the focal length decreases. It is worth noting that the results for $f = 75$ mm and $f = 100$ m are comparable because of their very close values of VED, as indicated in Table 3. Consequently, the higher spark energy densities, reached when the focal length decreases, allow the kernel to be more resistant toward the disruptions induced by the turbulent flow. This phenomenon explains the decrease of the MIE and the increase of the $u'_{critical}$ observed when the focal length is reduced.

3.4. Statistical study of the temporal evolution of the CH emission intensity of the flame kernel

To better describe the phenomenon of ignition transition in turbulent mixtures, a statistical analysis of the signal recorded by the photomultiplier tube (PMT) is performed. As it was explained in the description of the experimental set-up, the PMT is placed 40 mm above the spark location and records the temporal evolution of the CH emission intensity of the flame kernel convected by the flow. The aim of the PMT is to provide information on the success or the failure of the ignition trials, in order to determine the MIE. Examples of signals recorded during successful ignitions in a laminar flow and in a highly turbulent flow ($u' = 2.05$ m/s) are respectively reported on Figs. 8(a) and 8(b). These recordings display that the shape of the signals also provide information on the structure of the flame kernel. Indeed, in a laminar flow, the signals of the PMT are similar from an ignition to another, whereas, in a highly turbulent flow, the structure of the flame kernel undergoes significant modifications leading to the recording of signals of very different aspects. Consequently, to study the influence of the turbulence on the structure of the flame kernel, a statistical analysis is performed on the duration of the signal Δt_{signal} and on the amplitude at the middle of the signal A_{signal}, as indicated on Fig. 8(a).

The evolution of the relative Root Mean Square (RMS) of Δt_{signal} and A_{signal} are plotted as a function of the velocity fluctuation, on Figs. 9(a) and 9(b), respectively. The relative RMS corresponds to the ratio RMS/average of the studied variable. These figures display a change in slope for a velocity fluctuation approximately equal to 1 m.s^{-1}, which is of the order of the critical velocity fluctuations characterizing the different ignition transitions, previously identified. This change in slope

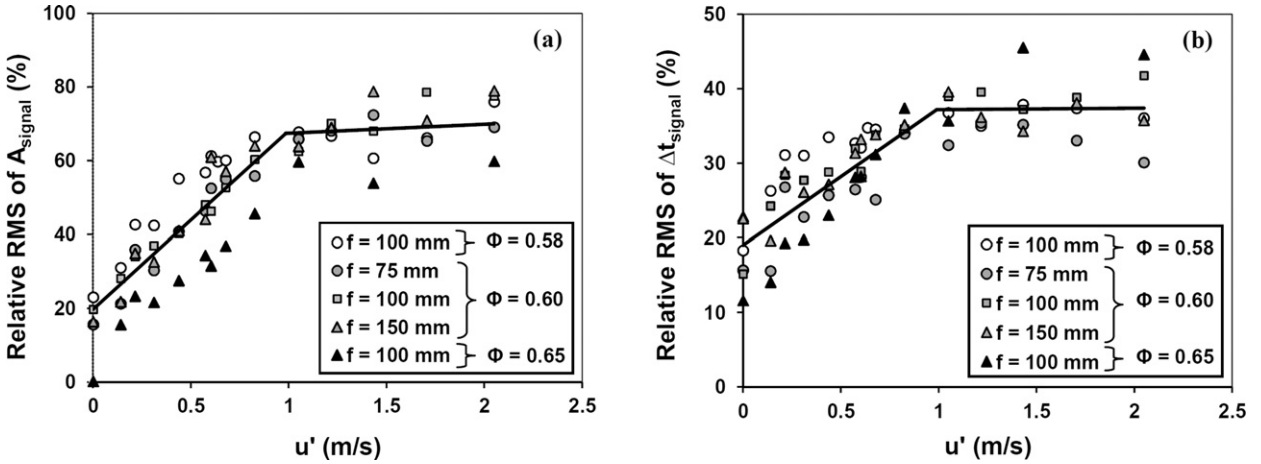

Fig. 9. Relative RMS of the amplitude A_{signal} (a) and the duration Δt_{signal}, (b) of the signal (temporal evolution of the CH emission intensity emitted by the flame kernel) recorded by the PMT, as a function of the velocity fluctuation.

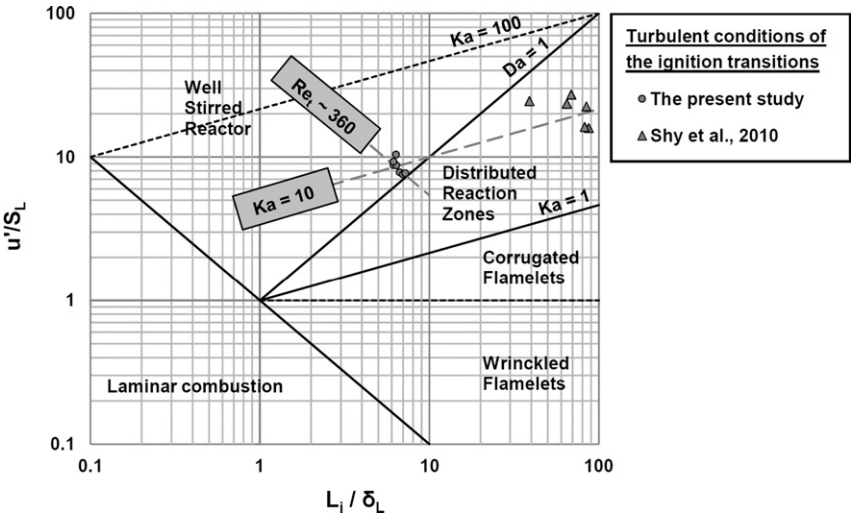

Fig. 10. Turbulent combustion diagram, displaying critical turbulence conditions observed in the present study and in that of Shy et al. [1].

confirms the existence of two distinct modes of flame structure at the origin of the ignition transition phenomenon. Before the regime change, the increase of the velocity fluctuation leads to rise the wrinkling of the flame front, which corresponds to a modification of the structure of the flame kernel at large scales. Thus, in this regime, the relative RMS increases as a function of the velocity fluctuation. Whereas, after the transition on Figs. 9(a) and 9(b), the relative RMS remains nearly constant, which means that, from a statistical point of view, the flame kernel displays the same properties at large scales. Indeed, in this regime, the wrinkling of the flame is already significant and the increase of the levels of turbulence leads to the modification of the thermal structure of the flame front at small scale, which cannot be recorded by the PMT.

Consequently, this statistical study of the signals recorded by the PMT during ignition confirms that a change in the flame structure occurs, from a certain threshold of turbulence. This phenomenon explains the transition observed in the evolution of the MIE as a function of the velocity fluctuation.

3.5. A common criterion for the ignition transitions

In order to find a common criterion for the ignition transitions previously observed, the critical turbulence conditions, for which an ignition transition occurs, are plotted on the turbulent combustion diagram, on Fig. 10. For the different equivalence ratios and volumes of energy deposition VED (function of the focal length), an ignition transition is observed for a Damköhler number lower than one and for a Karlovitz number of the order of 10. The calculation of the turbulent Reynolds number $Re_t = (u'.L_i)/\nu$, where ν is the kinematic viscosity of fresh gases mixture, reveals that, whatever the equivalence ratio and the VED, ignition transitions occur from a sufficiently high level of turbulence, corresponding to a constant turbulent Reynolds number of the order of 360.

The common criterion chosen for the different ignition transitions is the $Ka \sim 10$. Indeed, the value of Karlovitz number is generally used to characterize the flame structure. According to the turbulent combustion diagram, when the Karlovitz number becomes higher than 1, Kolmogorov scales are able to thicken the flame preheat zone, leading to intense stretch and possibly local extinctions. However, numerous studies [18–20] explain that a significant change in the combustion regimes is actually observed for a Karlovitz number, which is an order of magnitude larger than the Klimov–Williams criterion $Ka = 1$. Thus, the Karlovitz number calculated at the transitions, which corresponds to a change in the flame structure and which is of the order of 10, is consistent which those studies. Moreover, it is also in good agreement with the values of the Karlovitz numbers observed by Shy et al. [1] at its several ignition transitions, as shown on Fig. 10 by triangles. Consequently, the phenomenon of ignition transition seems to be universal, as a common criterion ($Ka \sim 10$) in turbulent mixtures can be found, whatever the experimental conditions.

4. Conclusion

To analyze the ignition through a spark of lean and highly turbulent premixed flows, laser-induced spark ignition of methane/air mixtures have been conducted and the MIE has been measured as a function of the turbulence intensity, the equivalence ratio and the volume of energy deposition (VED). The measurements have revealed that a higher MIE is required when the turbulence is more intense, when the VED increases and when the equivalence ratio of the lean mixture decreases. These trends are in good agreement with previous studies [1,2,10,11,17].

The measurements also display an ignition transition phenomenon, which is reported for the second time, but for different flow conditions and turbulence properties, and for a different ignition system, than Shy et al. [1]. Indeed, the MIE measurements as a function of u' describes linear slopes, with a slope breakdown (for $u' \sim 1$ m/s) which could be due to the transition between two distinct modes of flame structures. Since the MIE is proportional to δ^3 [15], an ignition transition occurs from a certain threshold of turbulence, because the flame kernel would not develop anymore in a flamelet regime, but in a regime where it would be strongly modified by the turbulence: the flame front would undergo a thickening by the small eddies ($Ka \sim 10$) and an intense mixing by all the eddies of the flow ($Da < 1$). Moreover, the statistical study of the signals recorded by the PMT during ignition confirms that a change in the flame structure occurs, when the turbulence intensity is raised.

This ignition transition in turbulent mixtures is also studied in others conditions, in terms of equivalence ratios and VED. This analysis reveals that an ignition transition happens for a more intense turbulence, when the equivalence ratio goes up and when the VED decreases.

Finally, this study reveals that there is a common criterion for the ignition transitions. Whatever the VED and the equivalence ratio of the mixture, an ignition transition occurs when the turbulent flow reaches a Karlovitz number of the order of 10. This value of the Karlovitz number, from which a change in the flame structure occurs, is consistent with the values reported in the literature [18–20]. Moreover, this criterion is also in good agreement with the ignition transitions recorded by Shy et al. [1]. Consequently, whatever, the ignition system (electric sparks or laser-induced sparks), the flow properties (cruciform explosion bomb or stationary flow) and the range of turbulence intensities, ignitions transitions are observed from the same value of the Karlovitz number ($Ka \sim 10$). This leads to the conclusion that the ignition transition in turbulent mixtures seems to be a more universal phenomenon.

References

[1] S.S. Shy, C.C. Liu, W.T. Shih, Combust. Flame 157 (2) (2010) 341–350.
[2] C.C. Huang, S.S. Shy, C.C. Liu, Y.Y. Yan, Proc. Combust. Inst. 31 (1) (2007) 1401–1409.
[3] Y. Huang, V. Yang, Prog. Energy Combust. Sci. 35 (2009) 293–364.
[4] N. Docquier, S. Candel, Prog. Energy Combust. Sci. 28 (2002) 107–150.
[5] A.H. Lefebvre, Gas Turbine Combustion, Taylor & Francis, 1999.
[6] J.R. Kee, M.E. Coltrin, P. Glarborg, Chemically Reacting Flows: Theory and Practice, John Wiley & Sons, 2003.
[7] B. Lewis, G. Von Elbe, Combustion Flames and Explosions of Gases, Academic Press, 1987.
[8] E. Mastorakos, Prog. Energy Combust. Sci. 35 (1) (2009) 57–97.
[9] D.R. Ballal, A.H. Lefebvre, Proc. Royal Soc. London Ser. A 357 (1977) 163–181.
[10] J.-L. Beduneau, B. Kim, L. Zimmer, Y. Ikeda, Combust. Flame 132 (4) (2003) 653–665.
[11] D.R. Ballal, A.H. Lefebvre, Proc. Combust. Inst. 15 (1) (1975) 1473–1481.
[12] N. Mazellier, L. Danaila, B. Renou, J. Turbul. 11 (2010) N43.
[13] G.F.W. Ziegler, E.P. Wagner, R.R. Maly, Proc. Combust. Inst. 20 (1984) 1817–1824.
[14] N. Otsu, IEEE Trans. Systems Man Cybern. 9 (1) (1979) 62–66.
[15] I. Glassman, Combustion, second ed., Academic Press, 1987.
[16] N. Peters, Turbulent Combustion, Cambridge University Press, 2000.
[17] T.X. Phuoc, F.P. White, Combust. Flame 119 (1999) 203–216.
[18] T. Poinsot, D. Veynante, S. Candel, J. Fluid Mech. 228 (1991) 561–606.
[19] W.L. Roberts, J.F. Driscoll, M.C. Drake, L.P. Goss, Combust. Flame 94 (1–2) (1993) 58–62.
[20] D. Bradley, Proc. Combust. Inst. 24 (1992) 247–262.